Human Molecular Genetics, 2006, Vol. 15, No. 4 ***569–579***
doi:10.1093/hmg/ddi473
Advance Access published on January 6, 2006

Multi-level regulation of myotubularin-related protein-2 phosphatase activity by myotubularin-related protein-13/set-binding factor-2

Philipp Berger[1], Imre Berger[2], Christiane Schaffitzel[2], Kristian Tersar[1], Benjamin Volkmer[1] and Ueli Suter[1,*]

[1]Institute of Cell Biology and [2]Institute of Molecular Biology and Biophysics, Department of Biology, Swiss Federal Institute of Technology ETH-Hönggerberg, CH-8093 Zürich, Switzerland

Received September 29, 2005; Revised December 8, 2005; Accepted January 4, 2006

Mutations in myotubularin-related protein-2 (*MTMR2*) or MTMR13/set-binding factor-2 (*SBF2*) genes are responsible for the severe autosomal recessive hereditary neuropathies, Charcot–Marie–Tooth disease (CMT) types 4B1 and 4B2, both characterized by reduced nerve conduction velocities, focally folded myelin sheaths and demyelination. MTMRs form a large family of conserved dual-specific phosphatases with enzymatically active and inactive members. We show that homodimeric active Mtmr2 interacts with homodimeric inactive Sbf2 in a tetrameric complex. This association dramatically increases the enzymatic activity of the complexed Mtmr2 towards phosphatidylinositol 3-phosphate and phosphatidylinositol 3,5-bisphosphate. Mtmr2 and Sbf2 are considerably, but not completely, co-localized in the cellular cytoplasm. On membranes of large vesicles formed under hypo-osmotic conditions, Sbf2 favorably competes with Mtmr2 for binding sites. Our data are consistent with a model suggesting that, at a given cellular location, Mtmr2 phosphatase activity is highly regulated, being high in the Mtmr2/Sbf2 complex, moderate if Mtmr2 is not associated with Sbf2 or functionally blocked by competition through Sbf2 for membrane-binding sites.

INTRODUCTION

Hereditary motor and sensory neuropathies, also called Charcot–Marie–Tooth (CMT) diseases, are among the most common inherited neurological disorders. Clinically, they are subdivided into two major groups on the basis of electrophysiological findings in peripheral nerves. Reduced nerve conduction velocity is observed in demyelinating neuropathies, whereas a reduction of the signal amplitude is found in axonal neuropathies (reviewed in 1). CMT4B1, an autosomal recessive hereditary neuropathy with early onset and severe progression, is caused by mutations in the myotubularin-related protein-2 gene *(MTMR2)* (2). Specific ablation of Mtmr2 in Schwann cells mimics the human disease in transgenic mice, indicating a glial origin of the disorder (3,4). Mutations in the related *MTMR13/*set-binding factor-2 *(SBF2)* gene lead to CMT4B2, a disease clinically and pathologically indistinguishable from CMT4B1 (5,6).

The myotubularin family is a large group of protein tyrosine/dual specificity phosphatase-like phosphatases. The founding member, myotubularin, is the disease-causing gene in X-linked myotubular myopathy (7). Fourteen family members have been identified in individual mammalian genomes, and homologs were found in all eukaryotes. Myotubularin-related proteins (MTMRs) contain an unusually large phosphatase domain, a pleckstrin homology-GRAM (PH-G) domain and a coiled-coil domain. Additional motifs include FYVE domains, pleckstrin homology (PH) domains and DENN domains (8,9). The phosphoinositides, PI-3-P and PI-3,5-P_2, are the major enzymatic substrates of MTMRs which remove the phosphate at the D3 position (10–12). Interestingly, not all MTMRs are active phosphatases. Six family members bear substitutions in catalytically essential amino acids of the phosphatase domain rendering them inactive. It has been speculated that these inactive phosphatases act as substrate traps protecting the substrate. Alternatively, they might be adaptor units for active MTMRs (13,14).

Mtmr2 is a 73 kDa protein in its monomeric form and exists as a dimer within cells (15). The recessive inheritance in CMT4B1 indicates loss-of-function mutations. This function

*To whom correspondence should be addressed. Tel: +41 16333432; Fax: +41 16331190; Email: usuter@cell.biol.ethz.ch

is likely to be the phosphatase activity because the tested disease-associated mutations in Mtmr2 lead to loss of phosphatase activity (11). Mtmr2 localizes to the cytosol under steady-state conditions, but the protein re-localizes to membranes in hypo-osmotic settings. The PH-G domain mediates this membrane association by binding to phosphoinositides (15). A similar re-localization was shown for myotubularin after EGF stimulation of COS cells (16). Sbf2 is an inactive phosphatase with a monomeric molecular weight of 208 kDa and contains a DENN domain and a PH domain, in addition to the basic MTMR motifs. PH domains are involved in membrane association and usually bind to PI-3,4-P_2 and/or PI-3,4,5-P_3 (17). The function of DENN domains is less well defined. Some of the DENN domain-containing proteins are involved in Rab and MAP kinase signaling, pointing to a function in vesicular trafficking and signaling processes (18).

The substrate specificity of active MTMRs suggests a function in endocytosis, sorting, and degradation of proteins, because PI-3-P and PI-3,5-P_2 are anchor sites on membranes for effector proteins of early and late phases of the endocytic process. PI-3-P is primarily produced by class III PI-3-kinase and is mainly localized on early endosomes. It recruits proteins with FYVE domains, such as EEA1 and Hrs, to this compartment. These proteins mediate important functions in the endocytic process (19,20). Endocytosis is blocked in *Caenorhabditis elegans* MTMR mutants functionally supporting a crucial role of MTMRs in this process (21). PI-3,5-P_2 is generated from PI-3-P by PIKfyve. PIKfyve localizes to late endosomes, indicating that this is the site of PI-3,5-P_2 production and function (22), although formal direct proof is lacking because the necessary specific tools are not yet available. The role of PI-3,5-P_2 in mammalian cells and the consequences of the putative modulatory effects of MTMRs on this substrate are enigmatic. Some hints have been provided by studies in yeast, which identified Ent3p, Ent5p, Vps24p and Svp1p as effectors of PI-3,5-P_2 (23–26). These proteins mediate various functions such as protein sorting into multivesicular bodies, heat tolerance and vacuole acidification. Thus, related processes might be regulated by mytobularins in higher eukaryotes. From a mechanistic point of view, dephosphorylation of PI-3,5-P_2 might be critical *per se*, or the product PI-5-P is the next signal in a signaling cascade.

Several interacting pairs of active and inactive MTMRs have been described. Myotubularin binds to MTMR12 (3-PAP), MTMR7 to MTMR9 and Mtmr2 to MTMR5/sbf1 (21,27–29). At least two major lines of evidence suggest a functionally critical interaction between Mtmr2 and Sbf2: (i) mutations in *MTMR2* and *SBF2* cause identical disease pictures in humans and (ii) MTMR5/sbf1, which interacts with Mtmr2, shares 58% amino acid sequence identity (74% similarity) with Sbf2. Here, we show that Mtmr2 and Sbf2 interact *in vitro* and *in vivo* in cultured Schwann cells and in myelinated peripheral nerves, the cell type and tissue that are the most relevant for the development of CMT4B. The purified Mtmr2/Sbf2 complex has an apparent molecular weight of ~600 kDa, indicating that two Mtmr2 polypeptides interact with two Sbf2 molecules, both in the form of homodimers. Binding of Sbf2 to Mtmr2 strongly increases the activity of Mtmr2 within the complex. Subcellular localization studies suggest that Sbf2 not only acts as an adaptor and activator for Mtmr2, but also as an independent competitive inhibitor of Mtmr2 localization and function.

RESULTS

Interaction of Mtmr2 and Sbf2

To test the potential association of Mtmr2 and Sbf2, we performed immunoprecipitation experiments with lysates from HEK293 cells stably expressing His-tagged Mtmr2 and/or HA-tagged Sbf2. These experiments showed that the two proteins physically interact (Fig. 1A), consistent with a very recent report (30). We also found Mtmr2/Sbf2 interactions between the endogenously expressed proteins in lysates from Schwann cell lines and sciatic nerve (Fig. 1B), the cell type and tissue that are affected in CMT4B. To examine whether Sbf2 is in a monomeric or an oligomeric state within cells, we performed immunoprecipitation experiments from cells that stably co-express HA- and VSV-tagged Sbf2. HA- and VSV-tagged proteins were found to interact, indicating the formation of Sbf2 oligomers (Fig. 1C).

To allow quantitative biochemical analysis and to gain first structural insight, we expressed and purified the His-tagged Mtmr2/Sbf2 complex in a baculovirus expression system that allows simultaneous expression of multiple proteins (31). A single NiNTA purification step, followed by gel filtration, yielded essentially pure Mtmr2/Sbf2 complex (Fig. 2A, inset). In addition, Mtmr2 is produced in excess in these cells and elutes as a dimer with an apparent molecular weight of 160 kDa. The observed molecular weight for the Mtmr2/Sbf2 complex is ~600 kDa, consistent with the interpretation that a dimer of Mtmr2 (146 kDa) interacts with a dimer of Sbf2 (416 kDa) (Fig. 2A). Association of two MTMR2/Sbf2 heterodimers [2 × (73 + 208 kDa)] remains a formal alternative (see what follows). We also attempted to express Sbf2 alone with the aim to analyze its oligomeric state. However, the protein was largely insoluble and co-expression of Mtmr2 was required for solubilization (data not shown).

To obtain an estimate of the overall dimensions, we analyzed the Mtmr2 dimer and the Mtmr2/Sbf2 complex by electron microscopy. The 146 kDa Mtmr2 appears as a compact particle with a diameter of ~10 nm, consistent with the dimensions calculated from the Mtmr2 crystal structure (32; Fig. 2B and C). The Mtmr2/Sbf2 complex is well structured and has approximately four times the size of the MTMR2 dimers, which is in agreement with the observed apparent molecular weight values (600 and 146 kDa, respectively). Some of the orientations of the complex suggest an X- or H-shaped reminiscent of a 2-fold symmetry (Fig. 2D).

We have previously shown that Mtmr2 forms homodimers via its coiled-coil domain (15). To elucidate the role of the coiled-coil domain of Sbf2, we generated a fusion protein consisting of maltose-binding protein (MBP) and the coiled-coil domain of Sbf2, connected by a TEV protease cleavage site in the linker. In gel filtration, the MBP–Sbf2cc fusion protein eluted at an apparent molecular weight of 110 kDa, indicating dimerization of the 58 kDa fusion protein (Fig. 3A). To confirm that the dimerization is mediated by the Sbf2 coiled-coil domain, we cleaved the MBP–Sbf2cc

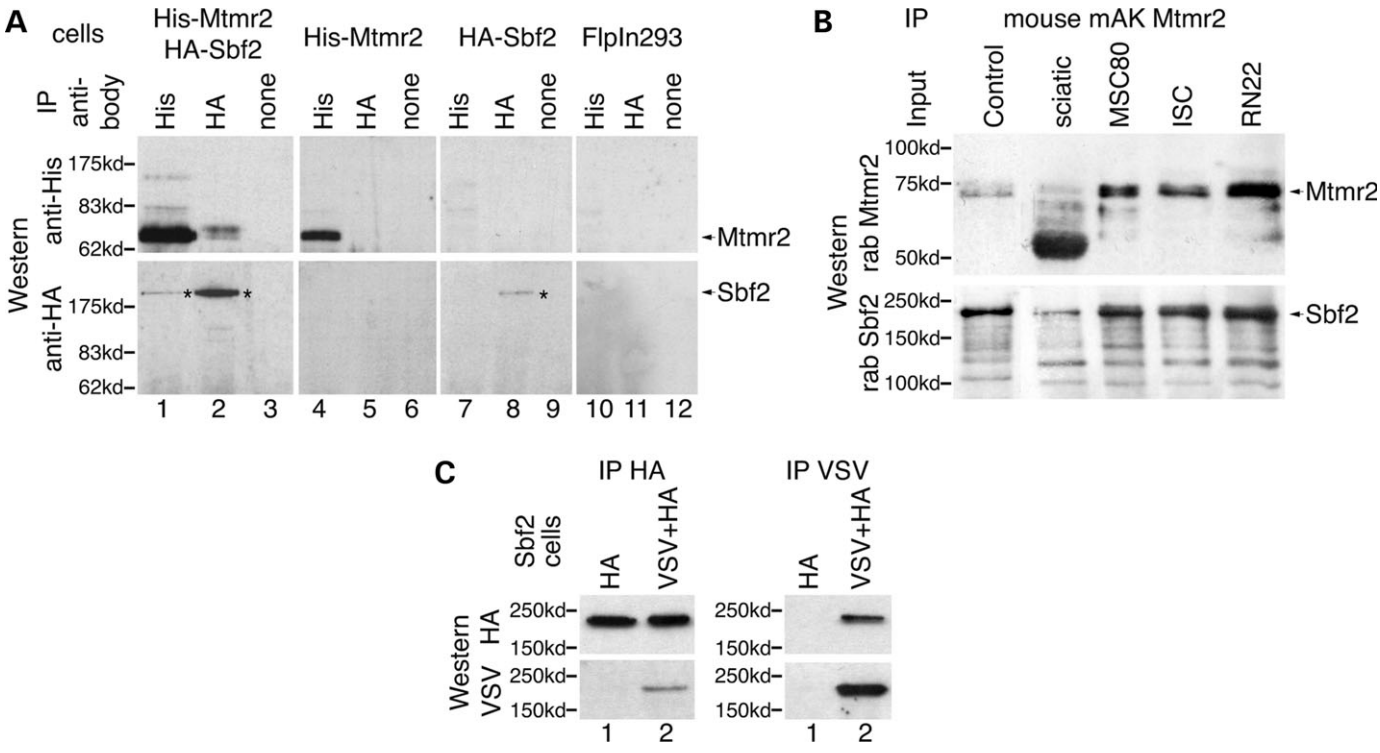

Figure 1. Sbf2 interacts with Mtmr2 and oligomerizes. (**A**) Immunoprecipitation from 293-FlpIn cells stably expressing His-tagged Mtmr2 and HA-tagged Sbf2 (panel 1). HA-tagged Sbf2 (asterisk) co-immunoprecipitates with His-tagged Mtmr2 (lane 1) and vice versa (lane 2). Immunoprecipitation from cells expressing His-tagged Mtmr2 (panel 2), HA-tagged Sbf2 (panel 3) and FlpIn293 (panel 4) cells were performed as controls. (**B**) Immunoprecipitation with monoclonal anti-Mtmr2 antibody and detection by western blotting with polyclonal rabbit anti-Mtmr2 (upper panel) and anti-Sbf2 (lower panel) antibodies. Mtmr2 is detected in sciatic nerve and in various Schwann cell lines. In sciatic nerve extracts, a degradation product of ~55 kDa was observed, besides the full-length form. Sbf2 is co-precipitated from sciatic nerve and Schwann cell lysates. Control: purified Mtmr2/Sbf2 complex (Fig. 2). Note that the levels cannot be quantitatively compared because less input lysate was used for the sciatic nerve. (**C**) Immunoprecipitation from 293-FlpIn cells stably expressing HA-Sbf2 (lane 1 in both panels) and HA- and VSV-tagged Sbf2 (lane 2). VSV-tagged Sbf2 co-immunoprecipitates with HA-tagged Sbf2 (left panel) and vice versa (right panel), indicating that Sbf2 exists within cells as an oligomer.

fusion protein with TEV protease and analyzed the products by gel filtration. After cleavage, MBP eluted as a monomer (apparent molecular weight of 43 kDa). The Sbf2 coiled-coil domain (15 kDa) eluted at ~30 kDa, consistent with dimerization (Fig. 3A). Thus, Sbf2 forms homodimers mediated by its coiled-coil domain.

It is intriguing to speculate how the coiled coils of Mtmr2 and Sbf2 are involved in tetramer formation (Fig. 3B). To address this issue, we used cell lines expressing HA-tagged Sbf2 and His-tagged Mtmr2. Although Mtmr2 and Mtmr2-C417S (the C417S mutation inactivates the phosphatase domain) interact with Sbf2, Mtmr2-P589X (coiled coil deleted) does not bind to Sbf2 (Fig. 3C). Conversely, when the coiled coil of Sbf2 was deleted, we found no interaction with Mtmr2 (data not shown). Hence, the coiled-coil domains are necessary to form two homodimers which then assemble independently of the coiled coils to a tetramer, or the interaction of Sbf2 and Mtmr2 occurs via a four-stranded coiled coil. Alternatively, two Mtmr2/Sbf2 heterodimers form via the coiled coils and assemble independently of the coiled coils to a tetramer (Fig. 3B). To examine these possibilities, we mixed MBP-Sbf2cc with a fusion protein of thioredoxin and the Mtmr2 coiled coil (Trx–Mtmr2cc). Trx–Mtmr2cc forms a stable dimer (15). An equimolar mixture of MBP–Sbf2cc and Trx–Mtmr2cc was analyzed by gel filtration (Fig. 3D). The two proteins eluted separately as homodimers without signs of tetramerization or heterodimerization. Altering the molecular ratios (2:1, 10:1 and 1:10) or incubating the proteins at 4 or 25°C also yielded no complexes of higher molecular weight. Partial thermal denaturation of the mixture at 50°C, followed by co-renaturation overnight, exclusively yielded homodimers. Finally, we incubated the MBP–Sbf2cc and Trx–Mtmr2cc mixture at 60°C, causing partial precipitation of MBP–sbf2cc. All remaining soluble MBP–Sbf2cc and all Trx–Mtmr2cc eluted after renaturation as homodimers. Thus, the homomeric interactions are extremely stable, excluding heterodimerization as well as tetramerization of the coiled-coil domains. Furthermore, a mixture of Mtmr2 dimer produced in insect cells and MBP–Sbf2cc dimer was analyzed by gel filtration, but no heterologous complex formation was observed (data not shown). We conclude that the coiled-coil domains exhibit their function in Mtmr2/Sbf2 tetramer formation indirectly by mediating homodimerization of Mtmr2 and Sbf2 (Fig. 3B, top).

Phosphatase activity

We have shown previously that bacterial GST-tagged and His-tagged Mtmr2 dephosphorylates PI-3-P and PI-3,5-P_2 at position D3 of the inositol ring. Other reports indicate that

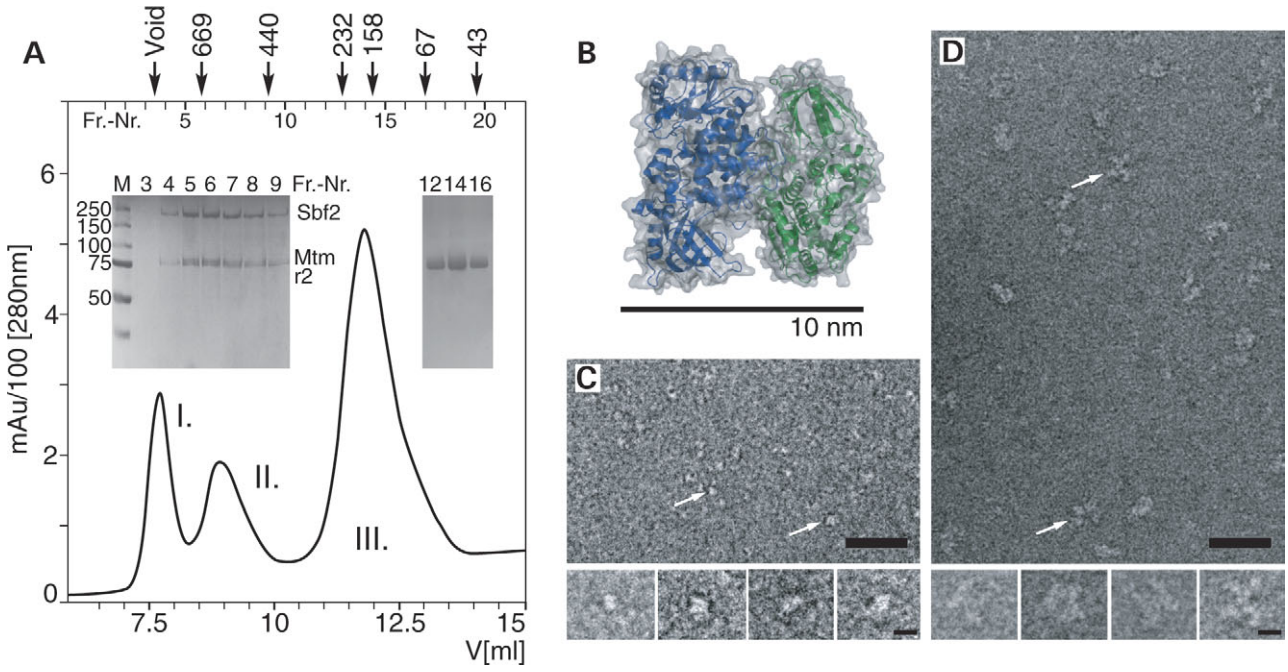

Figure 2. The Mtmr2/Sbf2 complex. (**A**) His-tagged Mtmr2 and CBP-tagged Sbf2 were expressed in sf21 cells, purified with NiNTA chromatography and analyzed by gel filtration. Peak I elutes with the void volume and does not contain proteins (large inset, lane 3). Peak II contains Mtmr2 and Sbf2 and elutes with an approximate molecular weight of 600 kDa, consistent with a $(Mtmr2)_2/(Sbf2)_2$ complex (calculated molecular weight: 570 kDa). Peak III elutes at an apparent molecular weight of 160 kDa and contains Mtmr2 homodimer, which is produced in excess in sf21 cells (small inset). (**B**) Crystal structure of the Mtmr2 dimer for size comparison (32). (**C**–**D**) Electron micrographs of negatively stained Mtmr2 and Mtmr2/Sbf2 complex. (C) Electron microscopic analysis of Mtmr2. Round particles with an approximate diameter of 10 nm were observed (arrows). (D) Electron micrographs of the Sbf2–Mtmr2 complex. X- or H-shaped particles with an ~4-fold larger size were seen (arrows). Beneath, four selected raw images with representative orientations are shown. Scale bars: 10 nm in B; 50 nm for overview pictures in C and D; 10 nm for magnifications in C and D.

probably all active MTMRs show this substrate specificity (10–12). Kim *et al*. (29) demonstrated, using separately purified proteins in a mixture that probably also contained uncomplexed Mtmr2 dimers, that the inactive phosphatase MTMR5/sbf1 increases the catalytic activity of Mtmr2. Our expression system and purification procedure yielded Mtmr2 dimer and Mtmr2/Sbf2 complex separately, providing us with the opportunity to measure the catalytic properties of pure Mtmr2/Sbf2 complex and pure Mtmr2 dimer independently. We found that both, Mtmr2 and Mtmr2/Sbf2 complex, use PI-3-P and PI-3,5-P_2 as substrates (Fig. 4). The activity towards PI-4-P, PI-5-P, PI-3,4-P_2, PI-4,5-P_2 and PI-3,4,5-P_3 was at background level (data not shown). The catalytic activity of Mtmr2 alone towards PI-3,5-P_2 was similar to the previously described activity (11). In contrast, the activity of the Mtmr2/Sbf2 complex is more than 25-fold increased. Similarly, the activity towards PI-3-P increases 10-fold upon Mtmr2/Sbf2 complex formation. The activity of the Mtmr2/Sbf2 complex towards PI-3,5-P_2 is approximately two times higher than towards PI-3-P (Fig. 4). Thus, the association of the inactive phosphatase Sbf2 with Mtmr2 is of paramount importance for the regulation of the specific Mtmr2 phosphatase activities towards PI-3,5-P_2 and PI-3-P.

Subcellular localization of Mtmr2 and Sbf2

The subcellular localization of MTMRs and its dynamics are of special interest in respect to the function of MTMRs. Mtmr2 localizes to the cytosol under steady-state conditions. Under hypo-osmotic conditions or after EGF stimulation of COS cells, Mtmr2 can bind as a dimer to membranes of late endosomes via its PH-G domain (15,16). It has been postulated that inactive mytobularin phosphatases regulate PI-3-phosphatase activity by targeting the active partner to the substrate (27,29). We analyzed the subcellular localization of Mtmr2 and Sbf2 in double-transfected COS cells in comparison with markers for vesicles of the endocytic pathway (Fig. 5). In Mtmr2/Sbf2 double-expressing cells, Mtmr2 is diffusely distributed in the cytosol as has been described for cells expressing Mtmr2 alone (15). Sbf2 is also present dispersed in the cytosol but the staining appeared more granular, comparable to cells expressing Sbf2 alone (data not shown). Mtmr2/Sbf2 stainings overlap considerably in line with the observed complex formation. No appreciable co-localization of Mtmr2 or Sbf2 with markers of early endosomes (EEA1), late endosomes (LBPA) or lysosomes (LAMP-2) was observed. Thus, despite the uneven distribution of Mtmr2 and, in particular, Sbf2 within the cells, these proteins are not strongly associated with these vesicles under resting conditions (Fig. 5). Under hypo-osmotic conditions, Sbf2 is redistributed to membranes of vacuoles formed in this setting. In contrast, no Mtmr2 staining was usually found on these vacuoles (Fig. 6A). Only cells with low Sbf2 expression show a co-staining of Mtmr2 and Sbf2 (Fig. 6B). This is surprising because cells on the same plate that only express Mtmr2 exhibit Mtmr2 vacuole membrane staining consistent with

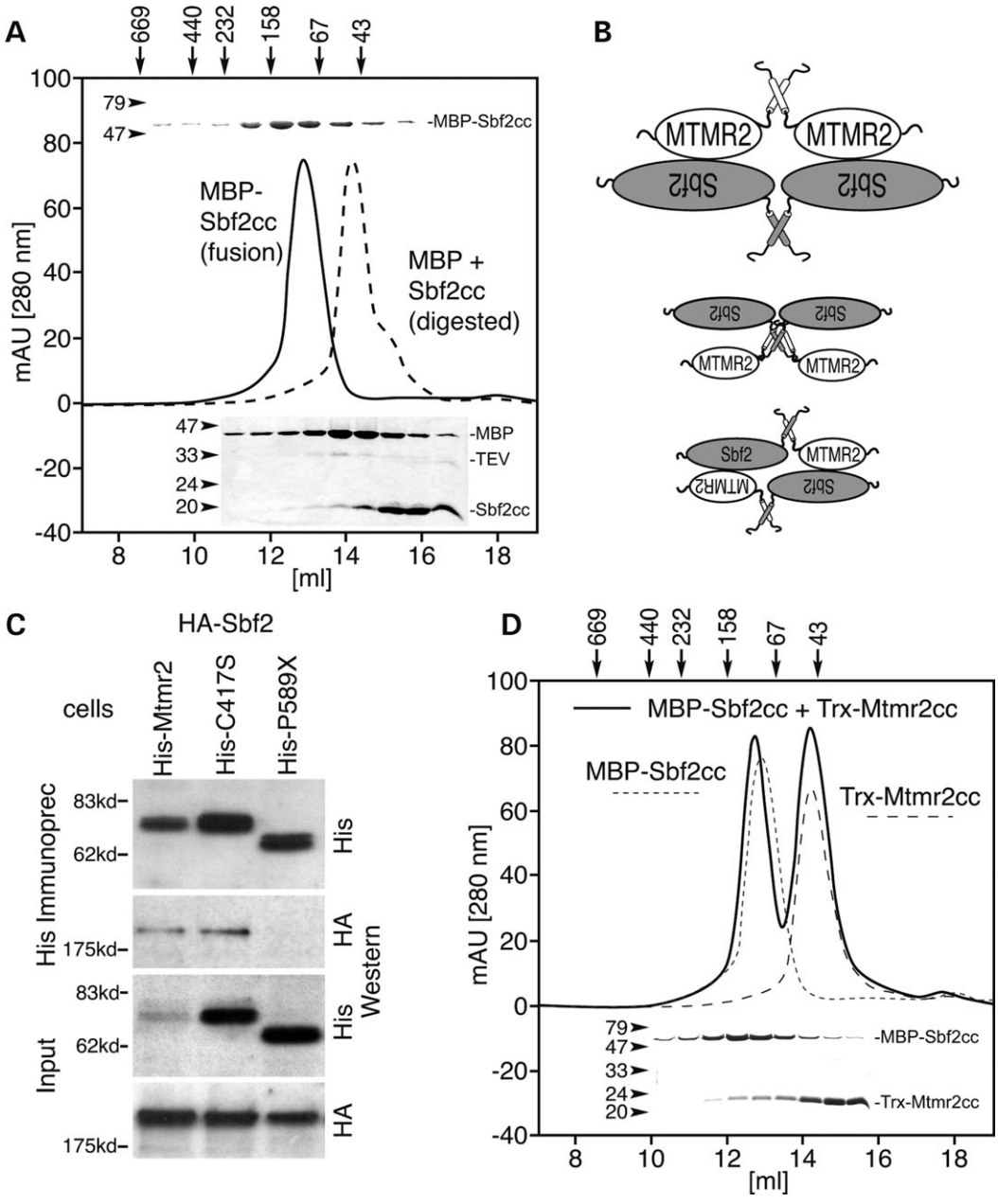

Figure 3. Function of the coiled coils of Sbf2 and Mtmr2. (**A**) Analysis of the coiled-coil region of Sbf2 fused to MBP with a TEV cleavage site in between (MBP–Sbf2cc, 58 kDa). Size exclusion chromatography revealed a molecular weight of ~110 kDa for the fusion protein, indicating that the coiled coil mediates dimerization (SDS–PAGE section on top). After cleavage with TEV protease between MBP (43 kDa) and the coiled coil (15 kDa), MBP elutes as a monomer and the coiled coil as a dimer (dotted line, SDS–PAGE analysis section at the bottom). (**B**) Putative forms of interactions between MTMR2 and Sbf2. (Top) Assembly of two homodimers. This model is in line with our data. (Middle) Two homodimers which form a four-stranded coiled coil. (Bottom) Two heterodimers forming the tetramer. (**C**) Immunoprecipitation experiments from FlpIn293 cells stably expressing HA-Sbf2 and His-Mtmr2 (lane 1), HA-Sbf2 and His-Mtmr2 C417S (w/o phosphatase activity, lane 2) and HA-Sbf2 and His-Mtmr2 P589X (w/o coiled coil, lane 3). Deletion of the coiled coil in Mtmr2 prevents the interaction with Sbf2. (**D**) Mixing of MBP–Sbf2cc (58 kDa) and the coiled coil of Mtmr2 fused to thioredoxin (Trx–Mtmr2cc, 20 kDa), both homodimers, yielded a mixture of the homodimers (solid line). Neither a 78 kDa peak indicative of a heterodimer nor a 156 kDa peak for a tetrameric assembly was observed (straight line, SDS–PAGE section at the bottom). The elution profiles of the fusion proteins applied separately are shown as dotted lines.

earlier observations (15) (Fig. 6D). We conclude that Sbf2 binds with considerably higher affinity than Mtmr2 to membranes of these vacuoles, thereby competing for Mtmr2-binding sites. This higher affinity can be mediated by the interaction of Sbf2 with membrane-binding proteins or membrane lipids (see what follows).

Lipid-binding properties of Sbf2

Sbf2 contains two putative lipid-binding domains, a PH-G domain and a classical PH domain. The PH-G domain was initially defined on the basis of primary sequence data, and the determination of the three-dimensional structure of

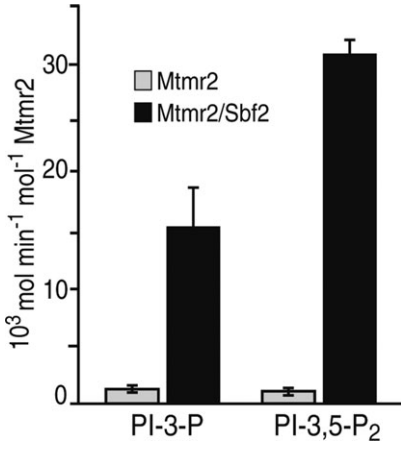

Figure 4. Phosphatase activity of Mtmr2 and Mtmr2/Sbf2 complex. The phosphatase activity was measured in a malachite green-based assay with di-C8 phosphoinositides as substrates. Only PI-3-P and PI-3,5-P_2 were dephosphorylated by Mtmr2 and the Mtmr2/Sbf2 complex. Association of Mtmr2 with Sbf2 strongly increases phosphatase activity. Please note that the activity of Mtmr2 expressed in a eurkaryotic system towards the substrates is similar to the previously described values for Mtmr2 expressed in a prokaryotic system.

Mtmr2 revealed a PH fold (32,33). This PH-G domain binds to phosphoinositides with broad specificity (15,16). We used a protein–lipid overlay assay to determine the lipid-binding properties of the PH-G domain of Sbf2 fused to an N-terminal GST tag (34) and found that the PH-G domain of Sbf2 binds to PI-4-P, PI-5-P, PI-3,5-P and PI-3,4,5-P_3 (Fig. 7A). This result is comparable to the findings with the PH-G domain of Mtmr2, indicating that this broad specificity might be common to PH-G domains, potentially defining a subclass within the large PH domain family. Interestingly, the PH domain at the C-terminus of Sbf2 shows specific binding only to PI-3,4,5-P_3 (Fig. 7B).

DISCUSSION

Mutations in *MTMR2* and *SBF2* lead to the clinically indistinguishable peripheral neuropathies, CMT4B1 and CMT4B2, respectively. This genetic hint and known associations of active and inactive MTMRs led us to investigate whether and how the active phosphatase Mtmr2 and the inactive phosphatase Sbf2 interact. We show that Mtmr2 and Sbf2 form a tetrameric complex composed of two homodimers. Association of Sbf2 with Mtmr2 strongly increases the enzymatic activity of the latter. The interaction between Mtmr2 and Sbf2 is tightly regulated, indicating that the individual proteins and the Mtmr2/Sbf2 complex play multiple roles within the cell.

The Mtmr2/Sbf2 complex

MTMRs form a large family of lipid phosphatases including both active and inactive members. Immunoprecipitation from transfected cells had revealed previously that some active and inactive members interact (27–29). Our initial experiments with cellular and tissue lysates showed that Mtmr2 and Sbf2 associate with each other. Thus, we produced and purified the Mtmr2/Sbf2 complex for biochemical analysis using MultiBac, a recently described baculovirus-based system for multi-protein applications (31). The expression levels of both Mtmr2 and Sbf2 were high when compared with previous experience with Mtmr2 expression in *E. coli*, demonstrating that eukaryotic systems offer significant advantages for efficient expression of MTMRs. We found that Sbf2 expressed alone is largely insoluble, suggesting that appropriate partners such as Mtmr2 are required for stabilization within cells. Co-expressed Mtmr2 and Sbf2 were isolated as a high molecular weight complex of ~600 kDa, most consistent with an association of an Mtmr2 dimer with an Sbf2 dimer to form a $(Mtmr2)_2/(Sbf2)_2$ complex. The existence of tetramers is further supported by electron microscopic analysis of the Mtmr2/Sbf2 complex, indicating an ~4-fold larger size as compared to the Mtmr2 dimer. The complex appears as X- or H-shaped particle consistent with speculations that the arms of the particle may be the N-terminal DENN and the C-terminal PH domains of Sbf2 because these are likely to form independent domains.

We assessed in two ways the function of the coiled-coil domains in Mtmr2 and Sbf2 in complex formation. Immunoprecipitation experiments revealed that deletion of the C-terminus containing the coiled coil of Mtmr2 or of Sbf2 abolished the interactions consistent with a recent publication (30). We then mixed the individual coiled coils of Mtmr2 and Sbf2 fused to thioredoxin and MBP, respectively, and found no indication of formation of heterodimeric or heterotetrameric complexes. Both coiled-coil proteins remained in or reformed their homodimeric state even after thermal unfolding followed by refolding. We conclude that the coiled-coil domains are not directly mediating the interaction between Mtmr2 and Sbf2. However, they are indirectly essential to mediate stable homodimerization (Fig. 3B, top). The interaction of Mtmr2 and Sbf2 in the complex must involve further domains, besides the coiled coils. In analogy, this might also hold true for other interacting pairs of active and inactive members of the myotubularin protein family. An attractive hypothesis would be that the phosphatase domain of Mtmr2 is involved in the formation of the Mtmr2/Sbf2 complex because the phosphatase activity is significantly upregulated upon complex formation.

Phosphatase activity and subcellular localization

Binding of Sbf2 to Mtmr2 increases the activity towards PI-3-P ~10-fold and towards PI-3,5-P_2 ~25-fold. This implies that complex formation drastically affects Mtmr2 phosphatase activity and causes a slight shift in substrate specificity. Understanding the biological significance of these findings is crucially important for the elucidation of the cellular roles of Mtmr2 and Sbf2. Mechanistic hints to this end were revealed by subcellular localization studies. In cells expressing Mtmr2 or Sbf2 alone, both proteins localize to the cytoplasm. Under hypo-osmotic conditions, vacuoles formed and Mtmr2 or Sbf2 accumulated at the membranes of these vesicles. A different picture emerged when Mtmr2 and Sbf2 were expressed in the same cell. We found a broad but incomplete overlap of Mtmr2 and Sbf2 in the cytoplasm. Hypo-osmotic conditions were applied, Sbf2 when bound to membranes of the formed vacuoles, whereas Mtmr2 remained in the cytoplasm. This intriguing preference for Sbf2 binding may reflect a higher affinity of the Sbf2 PH-G domain to phosphoinositides when

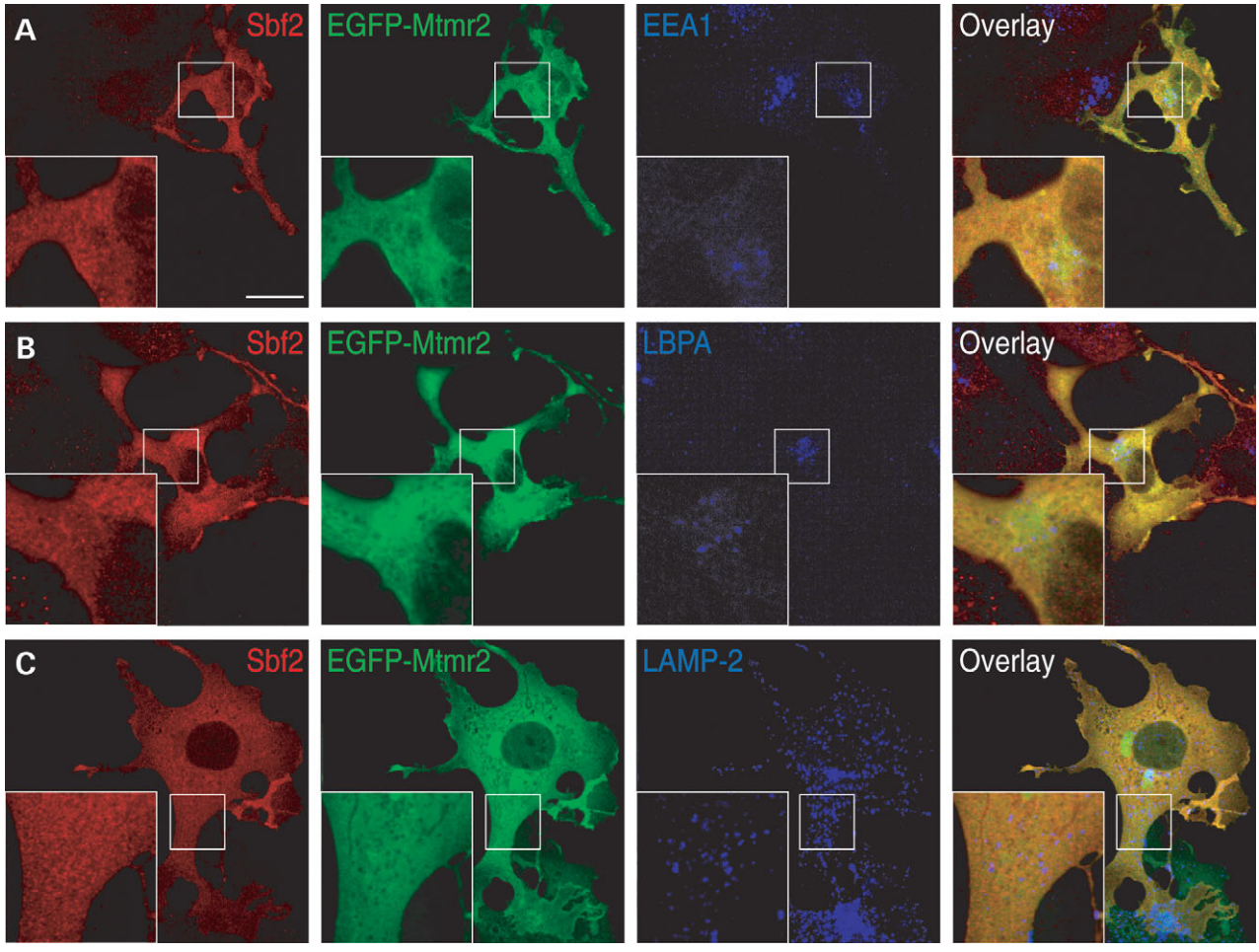

Figure 5. Subcellular localization of Mtmr2 and Sbf2. COS cells were co-transfected with Sbf2 and EGFP-Mtmr2 expression constructs and stained with markers for early endosomes (EEA1), late endosomes (LBPA) and lysosomes (LAMP-2). In double-expressing cells, both Mtmr2 and Sbf2 are diffusely distributed in the cytosol and do not co-localize appreciably with these vesicular markers under resting conditions. Scale bar: 20 μm.

compared with the Mtmr2 PH-G domain. Alternatively, other domains of the proteins or additional unknown factors might be involved. The PH domain of Sbf2 is an attractive candidate to play a role in this context, but this requires experimental confirmation. The distinct localizations of Mtmr2, Sbf2 and the Mtmr2/Sbf2 complex suggest an intriguing multi-level model for the regulation of Mtmr2 phosphatase activity. (i) The activity is maximal in defined regions of the cytoplasm where the Mtmr2/Sbf2 complex is located. (ii) Moderate activity is associated with the Mtmr2 dimer in the cytoplasm, or if the protein is bound to particular membranes in the absence of Sbf2. (iii) Mtmr2 phosphatase activity can be blocked at particular membranes owing to competition with Sbf2 for binding sites. Under resting conditions, the Mtmr2/Sbf2 complex likely degrades PI-3,5-P_2 (and/or PI-3-P) with maximal efficiency, which may explain the low cellular levels of PI-3,5-P_2. Complexes between active and inactive MTMRs might downregulate PI-3,5-P_2 levels in mechanistically similar ways in many different cell types, as MTMRs are ubiquitously expressed.

PI-3,5-P_2 levels transiently rise upon stimulation of cells with hypo-osmotic shock, EGF or interleukin-2 (16,35,36). Such an effect can be achieved either by transient production of the substrate or by protecting it from degradation. A protective function was initially postulated for the inactive MTMR5/sbf1 in the context of phosphorylated proteins (13). Our results suggest that inactive MTMR phosphatases have functions as (i) adaptors for the correct localization of active MTMRs, (ii) protectors of PI-3,5-P_2 and (iii) regulators of phosphatase activity of the active MTMR partners.

Implications for human disease

The correct function of MTMRs is crucial for human health. Mutations in three of the 14 family members cause hereditary human diseases. Mutations in myotubularin lead to X-linked myotubular myopathy, and mutations in either *MTMR2* or *SBF2* lead to the severe peripheral neuropathies, CMT 4B1 and 4B2, respectively (3,5–7). MTMR2 is an active phosphatase which dephosphorylates PI-3-P and PI-3,5-P_2 and loss of catalytic activity correlates with CMT4B1 (11). Sbf2 is an inactive phosphatase of the myotubularin family and all disease-associated mutations known to date lead to shortened or truncated proteins, also implicating loss-of-function.

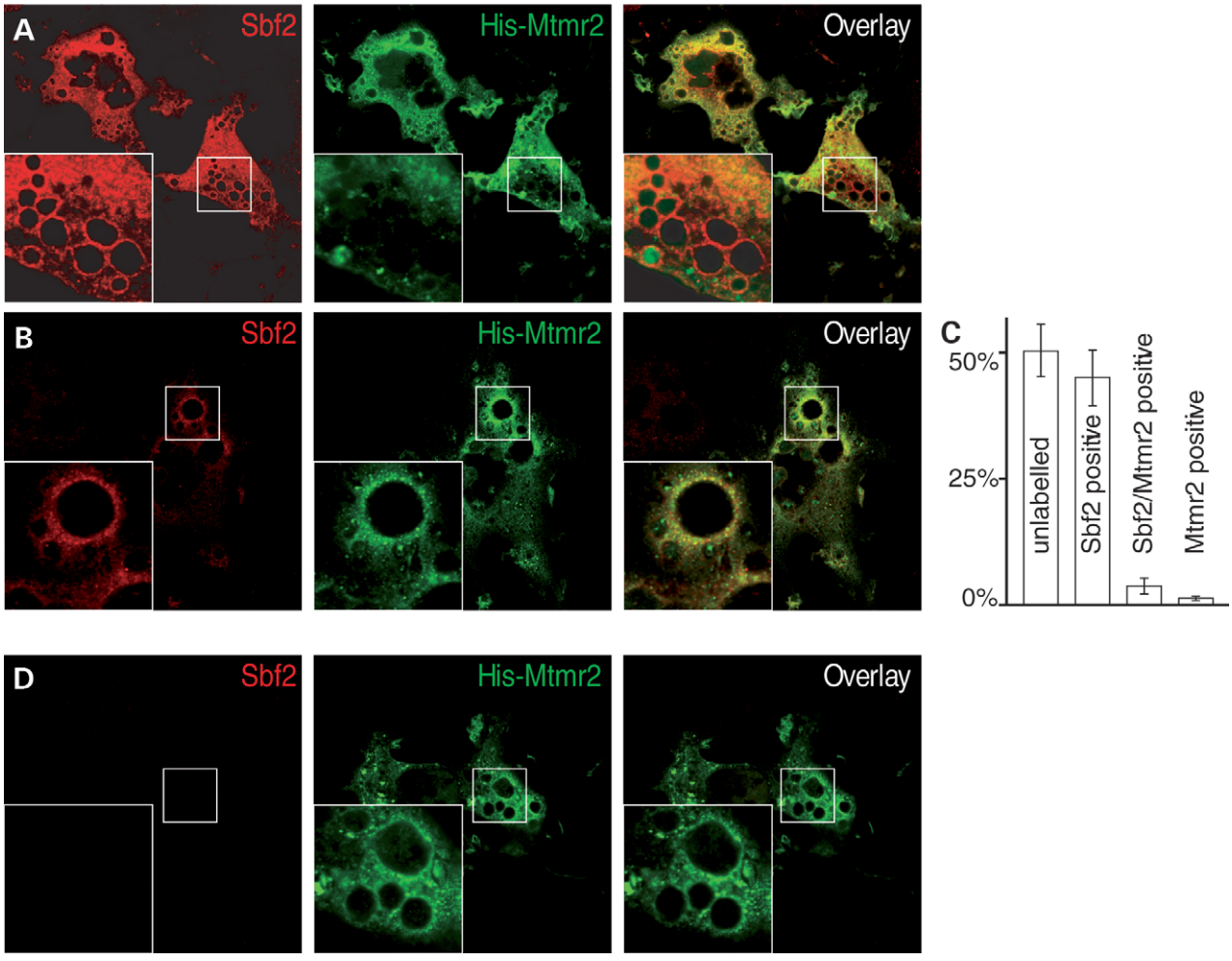

Figure 6. Subcellular localization of Mtmr2 and Sbf2 under hypo-osmotic conditions. COS cells were co-transfected with Sbf2 and His-Mtmr2 expression constructs. All pictures are from the same plate. (**A**) In cells expressing high levels of Sbf2, Sbf2 preferentially binds to the membrane of vesicles. (**B**) In cells with moderate Sbf2 expression, both Mtmr2 and Sbf2 bind to vesicles. (**C**) Quantification of labeled vesicle in double-expressing cells. 'Sbf2-positive' indicates percentage of vesicles labeled only for Sbf2, 'Mtmr2-positive' denotes percentage of vesicles labeled for Mtmr2 only and 'Sbf2/Mtmr2-positive' stands for percentage of double-labeled vesicles. Three times 100 vesicles in double-expressing cells from three independent experiments have been counted. (**D**) In cells which only expresses Mtmr2, Mtmr2 localizes to the vesicular membrane, as previously described in single-transfected cells (15). In single Sbf2-transfected cells under hypo-osmotic conditions, Sbf2 is also localized on the newly formed vesicles (data not shown).

Experiments in transgenic mice have shown that the Schwann cell-specific function of Mtmr2 is critical for the disease (3,4). We demonstrate that Mtmr2 and Sbf2 are interaction partners in Schwann cells *in vitro* and *in vivo*. This interaction is most likely the molecular basis for the identical phenotypes caused by mutations in Mtmr2 and Sbf2, indicating that these proteins act in concert in a bottleneck of an important pathway. Our data suggest that loss of Mtmr2/Sbf2 complex function, involving lack of maximal phosphatase activity, is responsible for the human disease. However, more subtle alterations in cellular physiology, as indicated by the complex interplay between Mtrm2 and Sbf2, remain to be considered as contributing factors.

Future aspects

Our ability to reconstitute the Mtmr2/Sbf2 complex recombinantly using baculovirus expression allows stochiometric, enzymatic and structural analysis. The system is expandable, and additional potential binding proteins can be added in the co-expression experiments. So far, MTMR5/sbf1, neurofilament light chain protein and SAP97 have been identified as additional binding partners of Mtmr2 (3,29,37). Future studies will reveal how these proteins bind to the Mtmr2/Sbf2 complex, whether they bind together or compete with each another and how they influence catalytic activity and complex localization.

MATERIALS AND METHODS

Cloning and antibodies

The mouse Sbf2 cDNA was obtained by assembling RT–PCR fragments generated from mouse brain and sciatic nerve RNA. The resulting sequence fitted with the consensus sequence of the available EST clones. Mutations and tags were introduced using a PCR-based strategy with Taq Plus Precision Polymerase

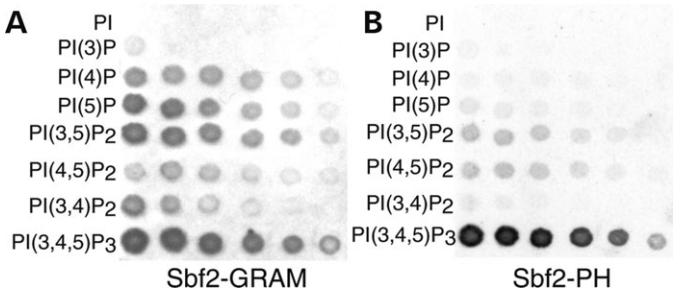

Figure 7. Protein–lipid overlay assay with the GST-tagged PH-G domain and the PH domain of Sbf2. (**A**) Serial dilutions of spotted phospholipids (100–3 pmol in 2-fold dilution steps from left to right) were incubated with the PH-G domain of Sbf2. A broad binding specificity is observed. (**B**) The PH domain of Sbf2 binds preferentially to PI-3,4,5-P_3.

(Stratagene). All constructs were verified by sequencing. The polyclonal anti-Sbf2 antiserum was obtained by immunizing rabbits with the peptide N-CKNKLLRASAPGDWES-C coupled to keyhole limpet hemocyanine (Pineda, Berlin). Production and characterization of monoclonal Mtmr2 antibodies will be described elsewhere.

Cell culture

For eukaryotic expression, the cDNA was cloned in the pcDNA3.1 zeo(+) and the pcDNA5/FRT vector. COS cells were transfected with Fugene6 (Roche) or Superfect (Qiagen) according to the manufacturer's recommendations. Stably expressing HEK293 FlpIn cells were produced by co-transfection of a pcDNA5/FRT vector with the Flp recombinase expression plasmid pOG44 followed by selection with hygromycin (FlpIn system, Invitrogen). Cells stably expressing two different proteins were produced by transfection of the described FlpIn cells with a pcDNA3.1 zeo(+) vector followed by selection with zeocin and hygromycin.

Immunoprecipitation

Approximately 400 cm^2 of stably transfected HEK293 FlpIn cells were removed from the plates with Lysis Buffer A (0.5% Triton X100, 100 mM NaCl, 50 mM Tris–HCl, pH 7.5). Cells were sonicated and cell debris removed by centrifugation. The supernatant was incubated for 2 h with 10 μl protein A Sepharose (Pharmacia) carrying either 1 μg mouse anti-RGSHis (Qiagen), 1 μg mouse anti-VSV (P5D4, Roche) or 0.5 μg rat anti-HA (3F10, Roche) antibody. The beads were washed three times with Lysis Buffer A. Bound proteins were separated on an 8% SDS–PAGE and identified by western blotting with anti-RGSHis, anti-VSV and anti-HA antibodies. As secondary antibodies, alkaline phosphatase-coupled goat anti-mouse and horse radish peroxidase-coupled rabbit anti-rat were used, followed by chemiluminescence detection.

Coiled-coil fusion constructs

The following primers were used to amplify the coding sequence for a TEV-site, the 125 amino acid long region between the phosphatase and PH domain of Sbf2 containing the coiled coil, and a C-terminal His-Tag: 5′-GATC GAATTC GAA AAC CTG TAT TTT CAG GGG GGA GGA GCT GGG CCC CAG-3′ and 5′-GATC TCTAGA TCA ATG GTG ATG GTG ATG GTG GTT CTT GGA TGT GTA CTG-3′. The fragment was cloned into the pMALc vector (NEB). The protein was expressed in *E. coli* Rosetta cells and purified via Amylose (NEB) and NiNTA (Qiagen) resin according to manufacturers' recommendations. The production of His-tagged thioredoxin fused to the coiled coil of Mtmr2 is described elsewhere (15).

Baculovirus expression and purification of Mtmr2 and Sbf2

The construct for the expression of His-tagged Mtmr2 under the control of the p10 promoter was generated by inserting an *Eco*RI (blunt ended)/*Sal*I fragment from the pQE30-Mtmr2 vector (15) into *Sma*I/*Xho*I cut pFBDM shuttle vector (31) resulting in pFBDM-Mtmr2. For dual expression of Mtmr2 and Sbf2, the cDNA for a calmodulin-binding protein (CBP)-tagged Sbf2 was inserted into MCS1 of pFBDM-Mtmr2 under the control of the polyhedrin promoter resulting in the dual expression vector pFBDM-Sbf2–Mtmr2. For expression of Sbf2 alone, the Mtmr2 expression cassette was excised from this dual vector with *Kpn*I and *Bss*HII. His-tagged Mtmr2 and CBP-tagged Sbf2 were co-expressed in sf21 cells as described (31). After centrifugation, cells were lysed by sonification in Lysis Buffer B (50 mM Tris–HCl, 100 mM NaCl, 0.5% Triton X100, 10 mM imidazole, 2 mM PMSF, Sigma protease inhibitor cocktail, pH 8.5). The cleared lysate was applied to an NiNTA column, washed and eluted with Lysis Buffer B with increasing concentrations of imidazole. The eluted complex contained Mtmr2 and Sbf2, as confirmed by western blotting with mouse anti-His and rabbit anti-Sbf2 antibodies (data not shown). In a complementary experiment, the lysate was bound to calmodulin-affinity resin, washed and then eluted with 50 mM Tris–HCl, 2 mM EGTA, 1M NaCl, 10 mM β-mercaptoethanol, pH 8.0. Western blotting also confirmed that the complex contained both Mtmr2 and Sbf2 (data not shown). The eluate of the NiNTA column was loaded on a Superdex S200 HR gel filtration column with 50 mM Tris–HCl, 100 mM NaCl, 0.01% Tween, pH 8.0, as elution buffer.

Negative-stain electron microscopy

Mtmr2/Sbf2 complex was purified from sf21 cells by NiNTA and calmodulin-affinity resin chromatography. Pure Mtmr2 dimer was obtained by NiNTA chromatography followed by gel filtration. Mtmr2 samples at 10 μg/ml and Sbf2-Mtmr2 samples at 12 μg/ml were adsorbed to glow-discharged carbon grids for 30 s, followed by washing with two drops of deionized water and staining with two drops of 1% uranyl acetate. Images were taken with a 2 k CCD camera at a magnification of ×53 000 and a defocus of 2 μM, using the low-dose procedure with a Philips TecnaiF20 electron microscope operated at 200 kV.

Phosphatase activity

Purified Mtmr2 dimer and Mtmr2/Sbf2 complex from sf21 cells were used for the activity assays. As substrates, diC8 phosphoinositides from Echelon were used (Malachite Green Phosphatase Assay Kit). Assays were performed at 30°C in a buffer containing 25 mM Tris–HCl pH 7.5, 5% glycerol, 2 mM DTT and 50 μM phosphoinositide. Aliquots were taken after 0.5–32 min and the reaction was stopped by adding *N*-ethylmaleimide to a final concentration of 7 mM and incubating at 95°C. Assays were performed with all seven phosphoinositides and their solubilization was tested by dephosphorylation with alkaline phosphatase in independent experiments.

Immunostainings

Cells were transfected as described previously and fixed 24 h after transfection with 2 or 0.5% paraformaldehyde in PBS. Hypo-osmotic conditions were applied as previously described (15). Cells were blocked in blocking buffer (10% FCS/0.05% Saponin/PBS) for 30 min prior to incubation with antibodies. Antibodies were diluted in blocking buffer as follows: mouse anti-EEA1 (1:300; BD Transduction Laboratories), mouse anti-LBPA (1:100; kindly provided by J. Gruenberg, Geneva), mouse anti-LAMP-2 (H4B4; 1:10; Developmental Studies Hybridoma Bank); mouse anti-RGSHis6 (1:200; Qiagen), rabbit anti-Sbf2 (1:1000). Appropriate Cy2, Cy3, Cy5 and ALEXA488 secondary antibodies were used for visualization.

Protein–lipid overlay assay

The predicted phosphoinositide-binding domains of Sbf2 were expressed in *E. coli* as fusion proteins with N-terminal GST tags. For the PH-G domain, the coding region of amino acids 864–1003 was amplified with Taq Plus Precision Polymerase (Stratagene) and cloned into the *Bam*HI/*Eco*RI cut pGEX-2T vector (Pharmacia). For the C-terminal PH domain, the coding region of amino acids 1719–1847 was cloned into the *Eco*RI cut pGEX-2T vector. The proteins were expressed and purified according to manufacturers' recommendations (Pharmacia). The protein–lipid overlay assay was performed with membranes from Echelon Biosciences (Salt Lake City), as previously described (15).

ACKNOWLEDGEMENTS

We thank Dr Ned Mantei for critical reading the manuscript, Dr Matthias Wymann for helpful discussions, Dr Jean Gruenberg for antibodies, Dr Rene Fischer for excellent help in the production of monoclonal antibodies and Liliane Diener for EM grids. I.B. was a Liebig Fellow of the Fonds der Chemischen Industrie (FCI, Germany). C.S. is supported by an Ernst Schering Research Foundation postdoctoral fellowship. This work was supported by the Swiss National Science Foundation and the National Competence Center in the research 'Neural Plasticity and Repair'.

Conflict of Interest statement. The authors declare that there is no conflict of interest.

REFERENCES

1. Suter, U. and Scherer, S.S. (2003) Disease mechanisms in inherited neuropathies. *Nat. Rev. Neurosci.*, **4**, 714–726.
2. Bolino, A., Muglia, M., Conforti, F.L., LeGuern, E., Salih, M.A., Georgiou, D.M., Christodoulou, K., Hausmanowa-Petrusewicz, I., Mandich, P., Schenone, A. *et al.* (2000) Charcot–Marie–Tooth type 4B is caused by mutations in the gene encoding myotubularin-related protein-2. *Nat. Genet.*, **25**, 17–19.
3. Bolino, A., Bolis, A., Previtali, S.C., Dina, G., Bussini, S., Dati, G., Amadio, S., Del Carro, U., Mruk, D.D., Feltri, M.L. *et al.* (2004) Disruption of Mtmr2 produces CMT4B1-like neuropathy with myelin outfolding and impaired spermatogenesis. *J. Cell Biol.*, **167**, 711–721.
4. Bonneick, S., Boentert, M., Berger, P., Atanasoski, S., Mantei, N., Wessig, C., Toyka, K.V., Young, P. and Suter, U. (2005) An animal model for Charcot–Marie–Tooth disease type 4B1. *Hum. Mol. Genet.*, **14**, 3685–3695.
5. Senderek, J., Bergmann, C., Weber, S., Ketelsen, U.P., Schorle, H., Rudnik-Schoneborn, S., Buttner, R., Buchheim, E. and Zerres, K. (2003) Mutation of the SBF2 gene, encoding a novel member of the myotubularin family, in Charcot–Marie–Tooth neuropathy type 4B2/11p15. *Hum. Mol. Genet.*, **12**, 349–356.
6. Azzedine, H., Bolino, A., Taieb, T., Birouk, N., Di Duca, M., Bouhouche, A., Benamou, S., Mrabet, A., Hammadouche, T., Chkili, T. *et al.* (2003) Mutations in MTMR13, a new pseudophosphatase homologue of MTMR2 and Sbf1, in two families with an autosomal recessive demyelinating form of Charcot–Marie–Tooth disease associated with early-onset glaucoma. *Am. J. Hum. Genet.*, **72**, 1141–1153.
7. Laporte, J., Hu, L.J., Kretz, C., Mandel, J.L., Kioschis, P., Coy, J.F., Klauck, S.M., Poustka, A. and Dahl, N. (1996) A gene mutated in X-linked myotubular myopathy defines a new putative tyrosine phosphatase family conserved in yeast. *Nat. Genet.*, **13**, 175–182.
8. Wishart, M.J. and Dixon, J.E. (2002) PTEN and myotubularin phosphatases: from 3-phosphoinositide dephosphorylation to disease. Phosphatase and tensin homolog deleted on chromosome ten. *Trends Cell Biol.*, **12**, 579–585.
9. Laporte, J., Bedez, F., Bolino, A. and Mandel, J.L. (2003) Myotubularins, a large disease-associated family of cooperating catalytically active and inactive phosphoinositides phosphatases. *Hum. Mol. Genet.*, **12**, R285–R292.
10. Walker, D.M., Urbe, S., Dove, S.K., Tenza, D., Raposo, G. and Clague, M.J. (2001) Characterization of MTMR3. An inositol lipid 3-phosphatase with novel substrate specificity. *Curr. Biol.*, **11**, 1600–1605.
11. Berger, P., Bonneick, S., Willi, S., Wymann, M. and Suter, U. (2002) Loss of phosphatase activity in myotubularin-related protein 2 is associated with Charcot–Marie–Tooth disease type 4B1. *Hum. Mol. Genet.*, **11**, 1569–1579.
12. Schaletzky, J., Dove, S.K., Short, B., Lorenzo, O., Clague, M.J. and Barr, F.A. (2003) Phosphatidylinositol-5-phosphate activation and conserved substrate specificity of the myotubularin phosphatidylinositol 3-phosphatases. *Curr. Biol.*, **13**, 504–509.
13. Cui, X., De Vivo, I., Slany, R., Miyamoto, A., Firestein, R. and Cleary, M.L. (1998) Association of SET domain and myotubularin-related proteins modulates growth control. *Nat. Genet.*, **18**, 331–337.
14. Nandurkar, H.H., Caldwell, K.K., Whisstock, J.C., Layton, M.J., Gaudet, E.A., Norris, F.A., Majerus, P.W. and Mitchell, C.A. (2001) Characterization of an adapter subunit to a phosphatidylinositol (3)P 3-phosphatase: identification of a myotubularin-related protein lacking catalytic activity. *Proc. Natl Acad. Sci. USA*, **98**, 9499–9504.
15. Berger, P., Schaffitzel, C., Berger, I., Ban, N. and Suter, U. (2003) Membrane association of myotubularin-related protein 2 is mediated by a pleckstrin homology-GRAM domain and a coiled-coil dimerization module. *Proc. Natl Acad. Sci. USA*, **100**, 12177–12182.
16. Tsujita, K., Itoh, T., Ijuin, T., Yamamoto, A., Shisheva, A., Laporte, J. and Takenawa, T. (2004) Myotubularin regulates the function of the late endosome through the GRAM domain- phosphatidylinositol 3,5-bisphosphate interaction. *J. Biol. Chem.*, **279**, 13817–13824.

17. Isakoff, S.J., Cardozo, T., Andreev, J., Li, Z., Ferguson, K.M., Abagyan, R., Lemmon, M.A., Aronheim, A. and Skolnik, E.Y. (1998) Identification and analysis of PH domain-containing targets of phosphatidylinositol 3-kinase using a novel *in vivo* assay in yeast. *EMBO J.*, **17**, 5374–5387.
18. Levivier, E., Goud, B., Souchet, M., Calmels, T.P., Mornon, J.P. and Callebaut, I. (2001) uDENN, DENN, and dDENN: indissociable domains in Rab and MAP kinases signaling pathways. *Biochem. Biophys. Res. Commun.*, **287**, 688–695.
19. Gaullier, J.M., Simonsen, A., D'Arrigo, A., Bremnes, B., Stenmark, H. and Aasland, R. (1998) FYVE fingers bind PtdIns(3)P. *Nature*, **394**, 432–433.
20. Simonsen, A., Lippe, R., Christoforidis, S., Gaullier, J.M., Brech, A., Callaghan, J., Toh, B.H., Murphy, C., Zerial, M. and Stenmark, H. (1998) EEA1 links PI(3)K function to Rab5 regulation of endosome fusion. *Nature*, **394**, 494–498.
21. Dang, H., Li, Z., Skolnik, E.Y. and Fares, H. (2004) Disease-related myotubularins function in endocytic traffic in *Caenorhabditis elegans*. *Mol. Biol. Cell*, **15**, 189–196.
22. Sbrissa, D., Ikonomov, O.C. and Shisheva, A. (2002) Phosphatidylinositol 3-phosphate-interacting domains in PIKfyve. Binding specificity and role in PIKfyve. Endomenbrane localization. *J. Biol. Chem.*, **277**, 6073–6079.
23. Friant, S., Pecheur, E.I., Eugster, A., Michel, F., Lefkir, Y., Nourrisson, D. and Letourneur, F. (2003) Ent3p Is a PtdIns(3,5)P2 effector required for protein sorting to the multivesicular body. *Dev. Cell*, **5**, 499–511.
24. Whitley, P., Reaves, B.J., Hashimoto, M., Riley, A.M., Potter, B.V. and Holman, G.D. (2003) Identification of mammalian Vps24p as an effector of phosphatidylinositol 3,5-bisphosphate-dependent endosome compartmentalization. *J. Biol. Chem.*, **278**, 38786–38795.
25. Eugster, A., Pecheur, E.I., Michel, F., Winsor, B., Letourneur, F. and Friant, S. (2004) Ent5p is required with Ent3p and Vps27p for ubiquitin-dependent protein sorting into the multivesicular body. *Mol. Biol. Cell*, **15**, 3031–3041.
26. Dove, S.K., Piper, R.C., McEwen, R.K., Yu, J.W., King, M.C., Hughes, D.C., Thuring, J., Holmes, A.B., Cooke, F.T., Michell, R.H. *et al.* (2004) Svp1p defines a family of phosphatidylinositol 3,5-bisphosphate effectors. *EMBO J.*, **23**, 1922–1933.
27. Nandurkar, H.H., Layton, M., Laporte, J., Selan, C., Corcoran, L., Caldwell, K.K., Mochizuki, Y., Majerus, P.W. and Mitchell, C.A. (2003) Identification of myotubularin as the lipid phosphatase catalytic subunit associated with the 3-phosphatase adapter protein, 3-PAP. *Proc. Natl Acad. Sci. USA*, **100**, 8660–8665.
28. Mochizuki, Y. and Majerus, P.W. (2003) Characterization of myotubularin-related protein 7 and its binding partner, myotubularin-related protein 9. *Proc. Natl Acad. Sci. USA*, **100**, 9768–9773.
29. Kim, S.A., Vacratsis, P.O., Firestein, R., Cleary, M.L. and Dixon, J.E. (2003) Regulation of myotubularin-related (MTMR)2 phosphatidylinositol phosphatase by MTMR5, a catalytically inactive phosphatase. *Proc. Natl Acad. Sci. USA*, **100**, 4492–4497.
30. Robinson, F.L. and Dixon, J.E. (2005) The phosphoinositide 3-phosphatase MTMR2 associates with MTMR13, a novel membrane-associated pseudophosphatase also mutated in type 4B Charcot–Marie–Tooth disease. *J. Biol. Chem*., **280**, 31699–31707.
31. Berger, I., Fitzgerald, D.J. and Richmond, T.J. (2004) Baculovirus expression system for heterologous multiprotein complexes. *Nat. Biotechnol.*, **22**, 1583–1587.
32. Begley, M.J., Taylor, G.S., Kim, S.A., Veine, D.M., Dixon, J.E. and Stuckey, J.A. (2003) Crystal structure of a phosphoinositide phosphatase, MTMR2: insights into myotubular myopathy and Charcot–Marie–Tooth syndrome. *Mol. Cell*, **12**, 1391–1402.
33. Doerks, T., Strauss, M., Brendel, M. and Bork, P. (2000) GRAM, a novel domain in glucosyltransferases, myotubularins and other putative membrane-associated proteins. *Trends Biochem. Sci.*, **25**, 483–485.
34. Dowler, S., Kular, G. and Alessi, D.R. (2002) Protein lipid overlay assay. *Sci. STKE*, PL6, 1–10.
35. Dove, S.K., Cooke, F.T., Douglas, M.R., Sayers, L.G., Parker, P.J. and Michell, R.H. (1997) Osmotic stress activates phosphatidylinositol-3,5-bisphosphate synthesis. *Nature*, **390**, 187–192.
36. Jones, D.R., Gonzalez-Garcia, A., Diez, E., Martinez, A.C., Carrera, A.C. and Merida, I. (1999) The identification of phosphatidylinositol 3,5-bisphosphate in T-lymphocytes and its regulation by interleukin-2. *J. Biol. Chem.*, **274**, 18407–18413.
37. Previtali, S.C., Zerega, B., Sherman, D.L., Brophy, P.J., Dina, G., King, R.H., Salih, M.M., Feltri, L., Quattrini, A., Ravazzolo, R. *et al.* (2003) Myotubularin-related 2 protein phosphatase and neurofilament light chain protein, both mutated in CMT neuropathies, interact in peripheral nerve. *Hum. Mol. Genet.*, **12**, 1713–1723.